Open access • Posted Content • DOI:10.1101/2021.09.13.460137

Convergent transcriptomic targets of propranolol and primidone identify potential biomarkers for essential tremor — Source link

Charles-Etienne Castonguay, Charles-Etienne Castonguay, Charles-Etienne Castonguay, Calwing Liao ...+8 more authors

Institutions: Montreal Neurological Institute and Hospital, McGill University, Université de Montréal

Published on: 15 Sep 2021 - bioRxiv (Cold Spring Harbor Laboratory)

Topics: Essential tremor and Pharmacogenomics

CONVERGENT TRANSCRIPTOMIC TARGETS OF PROPRANOLOL AND PRIMIDONE IDENTIFY POTENTIAL BIOMARKERS FOR ESSENTIAL TREMOR

Charles-Etienne Castonguay,[1,2,3] Calwing Liao,[1,2] Anouar Khayachi,[2] Gabrielle Houle[1,2], Jay P Ross,[1,2] Patrick A Dion,[2] Guy A Rouleau[2]

1 Department of Human Genetics, McGill University, Montréal, QC, Canada

2 Montreal Neurological Institute, McGill University, Montréal, QC, Canada

3 Faculté de Médecine, Université de Montréal, Montréal, QC, Canada

Corresponding author : guy.rouleau@mcgill.ca

ABSTRACT

Essential tremor (ET) is one of the most common movement disorders, affecting nearly 5% of individuals over 65 years old. Despite its high heritability, few genetic risk loci for ET have been identified. Recent advances in pharmacogenomics have generated a wealth of data that led to the identification of molecular signatures in response to hundreds of chemical compounds. Among the different forms of data, gene expression has proven to be quite successful for the inference of drug response in cell models. We sought to leverage this approach in the context of ET where many patients are responsive two drugs: propranolol and primidone. Propranolol- and primidone-specific transcriptomic drug targets, as well as convergent gene targets across both drugs, could provide insights into the pathogenesis of ET and identify possible targets of interest for future treatments. In this study, cerebellar DAOY and neural progenitor cells were treated for 5 days with clinical concentrations of propranolol and primidone, after which RNA-sequencing was used to identify differentially expressed genes. The expression of genes previously implicated in genetic and transcriptomic studies of ET and other movement disorders, such as *TRAPPC11*, were significantly upregulated by propranolol. Pathway enrichment analysis identified multiple terms

related to calcium signalling, endosomal sorting, axon guidance, and neuronal morphology. Convergent differentially expressed genes across all treatments and cell types were also found to be significantly more mutationally constrained, implying that they might harbour rare deleterious variants implicated in disease. Furthermore, these genes were enriched within cell types having high expression of ET related genes in both cortical and cerebellar tissues. Altogether, our results highlight potential cellular and molecular mechanisms associated with tremor reduction and identify relevant genetic biomarkers for drug-responsiveness in ET.

INTRODUCTION

Essential tremor (ET) is one of the most common movement disorders[1] affecting around 5% of individuals over 65 years old. The disease causes a 8-12 Hz kinetic tremor that typically affects the upper limbs but can also affect the head, voice, and rarely the lower limbs. Tremor intensity can sometimes increase with age and have a severe impact on activities of daily living. Recent studies aimed at identifying common and rare genetic variants have yielded mixed results, possibly due to clinical heterogeneity thus decreasing power of genetic studies[2]. Only a handful of variants have been identified and even fewer of them were replicated in other studies. Therefore, new approaches are needed, and transcriptomics might yield new insights in the pathophysiology of ET.

Recent studies in psychiatric genetics have successfully used drug effect screens to identify putative disease genes[3,4]. This approach is particularly relevant to diseases that have specific drug-responsive subsets of patients, as is the case with lithium responsive patients in bipolar disorder

(BD)[5]. This kind of approach has yet to be used in many drug-responsive neurological disorders such as ET where patients respond to two drugs: propranolol and primidone[6].

Propranolol and primidone are the most common drug treatments for ET. Both are efficient at reducing tremor by about 50% in ET patients[6]. Drug response is variable between patients, with some having a better outcome with either propranolol or primidone. Interestingly, some patients respond better to a combination of both drugs, especially for reducing limb and head tremors, hinting at potential additive or synergistic effects[7]. Propranolol is a beta-adrenergic receptor 1/2 antagonist initially developed to treat hypertension. In the context of ET, propranolol is thought to act on peripheral beta-2 receptors in muscle spindles, but it also has effects on cells in the central nervous system (CNS)[7,8]. Propranolol is lipophilic enough to cross the blood brain barrier (BBB) and to accumulate in high concentrations in mouse cerebellum and cortex following treatment[9]. Primidone is an anticonvulsant whose mechanism of action in ET is not well defined but it possibly reduces calcium and sodium currents across neuronal membranes[6], therefore, reducing neuronal excitability.

The transcriptomic effects of primidone and propranolol in the context of ET remain poorly understood[10,11]. Propranolol increased the expression *SHF*, a gene that was shown to be downregulated in ET patient cerebellum[10]. Studying the effects of tremor-reducing drugs on transcription can inform us on mechanisms that reduce tremors. Furthermore, it is possible that genes that are targeted by both drugs are implicated in ET pathophysiology and could allow for the identification of genes harbouring putative ET causing variants.

In this study, we identified convergent transcriptomic targets of primidone and propranolol in cortical neural progenitor cells (NPC) and cerebellar medulloblastoma cells (DAOY). Common cellular pathways affected by both treatments were related to neuronal morphology, axon guidance as well as cell-cell interactions as revealed by co-expression and pathway enrichment analysis. We also found that ET drugs specifically affected the expression of genes intolerant to loss-of-function (LoF) variants, hinting at possible enrichment of such rare LoF variants. Furthermore, with integration of single-cell data, we find that drug-targeted genes are mostly enriched in non-neuronal cell types such as endocytes, astrocytes, and oligodendrocytes in both cortical and cerebellar tissues. Our study identifies new putative ET- and tremor-related genes and informs on the molecular and cellular basis for tremor-reduction in ET.

METHODS

Cell culture and drug treatment

DAOY and NPC cells were cultured as previously described[5,11] and treated for 5 days with 20 ng/mL of propranolol or 5 µg/mL of primidone (n = 3 per treatment/cell line). H2O- or DMSO (0.023%)-treated cells were used as controls for propranolol and primidone, respectively. Drug concentrations were chosen based on previous studies that tested efficient tremor-reducing serum levels of propranolol and primidone in ET patients[12,13]. A kill curve was used to determine lethal drug concentrations for DAOY cells and NPCs in culture (Supplementary Table 10-12, Supplementary Figure 1-2).

RNA-sequencing and differential expression analysis

RNA was extracted with the RNeasy Mini Kit (Qiagen). cDNA library preparation was done using NEBNext stranded library preparation protocol (New England Biolabs) with rRNA depletion using the QIAseq FastSelect rRNA HMR kit. (Qiagen). Samples were sequenced on the Illumina NovaSeq6000 platform (150bp paired-end reads, 150M reads). FASTQ files were pseudo-aligned to the Ensembl v102 annotation of the human genome using Salmon v1.4.0[14]. Gene-level differential expression analysis was done using the R package Sleuth[15]. Only genes with a minimum of 10 scaled reads per base in 90% of samples were kept to filter out low-count genes. Cell types and treatments were analyzed separately using the Wald test (WT). The full model for the WT was:

$$Differentially\ expressed\ genes\ (DEG) \sim plate + buffer + treatment$$

MA plots and p-value histograms displayed expected distributions (Supplementary Figure 3,4). Meta-analysis of gene Z-scores was performed to analyze convergent DEG across cell types and treatments. Briefly, Z-scores for each gene were calculated and then summed across different combinations of cell types and treatments using Stouffer's Z method[16]. Multiple analyses were performed notably propranolol specific effect across cell types (labeled 'prop'; Supplementary table 6), primidone effect across cell types ('prim'; Supplementary table 7), convergent propranolol and primidone effect in each cell type ('daoy' and 'npc'; Supplementary tables 8 and 9 respectively) and convergent primidone and propranolol effects across both cell types ('all'; Supplementary table 5). False discovery rate was controlled for using the Benjamini-Hochberg procedure (q-value threshold < 0.05). At least 3 DEGs with highest fold-change per condition were validated using TaqMan qPCR probes (Supplementary Table 13).

WGCNA, co-expression and pathway enrichment

WGCNA was done using the R package[17]. DAOY and NPC sequencing results were analyzed separately, merging both primidone and propranolol treatments in the analysis. Normalized TPM values obtained from Sleuth ('sleuth_to_matrix') were used for the analysis. To filter out noisy low-count genes, only genes with a minimum of 10 TPM in 47% of samples were kept, for a final list of 8549 genes in DAOYs and 9260 genes for NPC. Two outlier samples ('DAOY_PRIM_03' and 'NPC_PRIM_02') were removed from the analysis based on sample clustering dendrogram. Fisher's exact test was used to calculate gene-module p-values. Co-expression analysis was performed using GeneNetwork2.0[18]. Pathway enrichment analysis was done using the gprofileR R package[19]. Briefly, gene-lists were made from convergent DEGs across multiple conditions (both drugs in DAOYs or NPCs, propranolol or primidone in both cells, both drugs in both cells). Custom background used in gprofiler comprised genes expressed in either DAOYs, NPCs or both when pertinent. The g:SCS algorithm was used for multiple testing correction (q-value threshold < 0.1).

Correlation with ET TWAS summary statistics

ET TWAS summary statistics were obtained from Liao et al. (2021; unpublished results). A generalized linear model was used to measure the strength of association between gene-level drug Z-scores and TWAS Z-scores, controlling for gene length and gene GC content ('lm' function in R). Weighted Z-scores were also used to account for significance of effect. The formula used were:

$$TWAS.Z = Drug.Z + Gene\ length + GC\ content$$

And for the weighted Z-score analysis:

$$TWAS.Z^2 = Drug.Z^2 + Gene\ length + GC\ content$$

Association p-values were corrected for multiple testing using Benjamini-Hochberg (q-value threshold < 0.05).

Single cell enrichment analysis

A one sample Z-test was used to test enrichment of drug-targeted genes as described previously[20]. An ET gene-set was curated from genes associated with ET from linkage, whole-exome, GWAS and transcriptomic studies [2,10]. Drug gene-sets were made from convergent DEGs (FDR < 0.05) across different conditions (DAOY, NPC, propranolol, primidone, all conditions). Adult cerebellum single-nucleus RNA sequencing data was obtained from Lake et al. (2018; GEO accession: GSE97930)[21]. Average cell counts per cell-type were obtained using Seurat v4.0.1[22]. Trimmed means per cell-type from adult cortex single-cell RNA-sequencing were obtained from the Allen Brain Atlas Smart-seq multiple cortical regions dataset[23]. To account for drop-out rates and reduce zero-inflation of the single-cell count matrices, low average count genes were filtered out in both cerebellum (< 0.5 counts in 7/10 cell types) and cortex (<1 count in 85/121 cell types). Single sample Z-tests were used to obtain cell-type specific enrichment Z-scores:

$$Z - score = \frac{Mean\ geneset\ counts - Mean\ cell\ type\ expression\ counts}{Geneset\ standard\ deviation * \sqrt{Number\ of\ genes\ in\ geneset}}$$

Loss-of-function analysis

The distribution of mutational constraint scores for drug DEGs was assessed using pLoF o/e ratio scores obtained from gnomAD[24]. pLof scores for convergent genes across all conditions with q-val <0.05 were compared all protein coding genes passing QC from the Sleuth differential expression analysis. To account for coding sequence length and gene GC percentage, propensity score matching with replacement was used (matchIT package in R[25]) to measure pLoF score

161 distribution differences between DE drug genes and all protein coding genes included in the meta-
162 analysis. Nearest neighbor matching with the maximum number of matches (ratio = 1:43) between
163 non-DEGs and DEGs was used. A Wilcoxon unpaired test was done on the matched data. The
164 same methods were used to assess pLoF score differences of upregulated (match ratio = 1:57) and
165 downregulated (match ratio = 1:178) DEGs with all protein coding genes.

166

167 **RESULTS**

168 **Differential expression following propranolol and primidone treatment**

169 To assess the transcriptomic effect of propranolol and primidone on neuronal and cerebellar cells,
170 NPCs and DAOYs were independently treated with clinically relevant concentrations of both
171 drugs for five days. Treatment of DAOYs with propranolol resulted in 1,754 DE genes
172 (Supplementary Table 1) while treatment of NPCs resulted in 1,571 DE genes (Supplementary
173 Table 2). Directionality of overall transcriptional effect was widely different between NPCs and
174 DAOYs, with propranolol treatment resulting in mostly overexpression in DAOYs and
175 underexpression in NPCs (Figure 1C and 1D). Pearson correlation of propranolol-treated NPCs
176 and DAOYs effectively show a strong negative correlation, indicating opposite transcriptomic
177 effects on the same genes ($r = -0.35$, p-val < 2.2E-308, Figure 1A). However, this correlation
178 weakens when weighing for the most significant DEGs ($r = -0.283$, $p = 7.1E-214$, Figure 1B).
179 Primidone, on the other hand, had a weak effect on transcription in both NPCs and DAOYs with
180 only 200 (Supplementary table 4) and 23 DEGs (Supplementary table 3) in each, respectively. In
181 NPCs, propranolol and primidone DEGs were lowly correlated ($r = -0.06$, p-val = 1.6E-11, Figure
182 1A) with a weaker weighted correlation ($r = -0.021$, p-val = 2.2E-02, Figure 1B). Similar weak

(weighted and unweighted) correlations are seen between the two drugs in DAOYs (Figure 1A and 1B).

ET drug targets converge on genes related to movements disorders and ET

Shared effects of propranolol and primidone on specific genes increases the likelihood of these genes being integral to tremor reduction in ET. Therefore, convergence of drug effects on expression was assessed by comparing gene Z-scores from different treatment conditions: convergent drug targets in either DAOYs or NPCs, convergent propranolol or primidone targets in both cell types and convergent targets of both drugs in all cell types.

Across DAOYs and NPCs, 788 significant convergent DEGs were found with propranolol treatment (Supplementary table 6) and 36 convergent DEGs following primidone treatment (Supplementary table 7). Propranolol, in both cell types, increased expression of *TRAPPC11*, a trafficking protein previously associated with ET[26] (z-score = 5.41, p-val = 5.87E-06). Propranolol also decreased expression of *G3BP1* (z =-9.07, q-val = 7.84E-17), which encodes a protein implicated in stress granule formation and is known to affect axonal mRNA translation as well as nerve regeneration[27]. *BRD2*, a transcription factor previously implicated with epilepsy, was upregulated following propranolol treatment in both cells (z = 21.13, q-val = 4.56E-95). *NONO* (z = 6.93, q-val = 3.69E-09), a gene harbouring a splicing variant known to cause X-linked intellectual deficiency with intentional tremor, was found to be upregulated[28]. Primidone, across NPCs and DAOYs, upregulated *VCAM1* (z-score = 5.53, p-value = 1.29E-04), a gene implicated in axonal myelination by oligodendrocytes[29]. *GIPC1* was also found to be downregulated following primidone treatment in both cell types (z = -5.46, q-val = 1.42E-04). GIPC1 is a known interactor of DRD3 which has previously been associated with ET and Parkinson's (PD)[2,30,31].

206

207 **Propranolol and primidone act on pathways related to neuronal survival as well as axon**
208 **guidance**

209 Following the identification of convergent DEGs across treatments, we wanted to identify
210 molecular pathways affected by propranolol and primidone in DAOYs and NPCs. Co-expression
211 enrichment analysis (using GeneNetwork2.0[18]) for convergent DEGs across all conditions showed
212 that Reactome terms related to GPCR signalling (p-val = 1.12E-19), axon guidance (p-val = 1.68E-
213 08), Semaphorin interactions (p-val = 3.24E-13) and VEGF signalling (p-val = 2.23E-08) were
214 significantly enriched within the convergent genesets (Supplementary Table 14). Furthermore,
215 Ca^{2+} signalling (p-val = 4.67E-07) and voltage-gated potassium channels (p-val = 4.64E-06) were
216 also found to be significantly enriched. Interestingly, GO:cellular components significant terms
217 were mostly related to cell:cell or cell:extracellular matrix interactions as well as axon guidance
218 such as lamellipodium (p-val = 4.47E-13), filopodium (p-val = 3.54E-11, focal adhesion (p-val =
219 4.70E-11) and growth cone (p-val = 1.04E-09)(Supplementary table 16).

220 Pathway enrichment analysis of convergent propranolol DEGs (in both cell types) was also
221 performed using g:profiler using genes expressed in both DAOYs and NPCs as background (Table
222 1). Pathways known to be affected by propranolol such as HIF-1α (p-val = 0.001) and regulation
223 of apoptosis (p-val = 0.02) were significantly enriched. Much like the co-expression analysis,
224 Reactome terms related to axon guidance were found to be significant, such as RUNX1
225 transcription (p-val = 0.0002), a transcription factor implicated in growth cone guidance of DRG
226 neurons[32]. Interestingly, CaMKK2 signalling pathway was found to be significantly enriched

227 within genes in the propranolol geneset. *CAMKK2* encodes a kinase implicated in synapse
228 homeostasis and is also involved in modyifing Aβ synaptotoxicity in Alzheimer's disease[33].

229 Weighted gene correlation network analysis was also performed to identify co-expression modules
230 associated with combined propranolol/primidone treatment. Module-trait and module correlation
231 heatmaps are shown in Figure 2. Two modules (cyan and red; corr = 0.74, p-val = 0.009; corr =
232 0.73, p-val = 0.01 respectively; Figure 2A) were found to be significantly associated with treatment
233 in DAOYs and only one module (red; corr = 0.65, p-val = 0.03) was significantly associated with
234 NPCs (Figure 2B). Pathway enrichment analysis of DAOY red module genes found an enrichment
235 of Reactome terms related to RABGAP signalling (p-val = 0.009) as well as RUNX1 transcription
236 (p-val = 0.02; Table 2). NPC red modules genes were significantly associated with neuronal
237 morphology, axon guidance and neurogenesis (Table 3).

238

239 **Correlation of the effects of propranolol and primidone with those of common and rare**
240 **variants in ET**

241 TWAS studies the effect of common SNPs associated with a disease on the expression of genes in
242 different tissues. We postulated that transcriptomic targets of propranolol and primidone might
243 correlate with the transcriptomic effect of common ET variants. We used TWAS summary statistic
244 from an upcoming ET GWAS (Liao et al., unpublished results) to measure the correlation between
245 TWAS gene Z-scores and convergent drug target Z-scores (across all possible conditions) while
246 controlling for gene length and GC content. Weak, non-significant correlations between TWAS
247 Z-scores and drug target Z-scores were found across all conditions and all brain tissues ($p > 0.05$;
248 Figure 3A). Cerebellar hemispheres and cerebellum tissues, brain regions highly associated with

ET, displayed non-significant negative correlations with convergent drug targets (coeff = -0.0143, p-val = 0.549; coeff = -0.000138, p-val = 0.994 respectively; Figure 3B).

We postulated that since propranolol and primidone had a non-significant correlation with expression of genes harbouring common variants for ET, they might instead act on genes that have rare variants. GnomAD recently published observed/expected (o/e) loss-of-function (LoF) scores for all protein coding genes in the genome. These scores inform on the tolerance of genes to rare LoF variants, with genes with a higher frequency of observed to expected LoF variants being more tolerant to mutations. Figure 3C shows the distribution of LoF scores of drug DEGs compared to all protein coding genes passing the initial DE QC. Drug targets displayed a significantly lower o/e score median (n = 256, median = 0.18) than all protein coding genes (n = 11,188, median = 0.36; W = 1727520, p-val = 1.501E-10) using a Wilcoxon unpaired test. Interestingly, when looking at fold change direction (figure 3D), upregulated genes (n = 194) had a significantly lower o/e score median (median = 0.15, W = 1361482, p-value = 2.917E-12) than all protein coding genes whilst no significant difference was found between o/e scores medians of downregulated genes (n = 71) and all protein coding genes (median = 0.35, W = 417126, p-value = 0.3246) using a Wilcoxon unpaired test. Thus, propranolol and primidone increased expression of mutationally constrained genes in cultured DAOYs and NPCs.

Single cell enrichment of propranolol and primidone targeted genes

Our current understanding of CNS cell types affected in ET is still very limited. Enrichment of disease related genes can indirectly inform on potential cell types implicated in disease

pathophysiology[20]. We first sought to assess the enrichment of ET genes discovered through familial linkage studies as well as whole-exome studies in cell types of the adult cerebellum and cerebral cortex (Figure 4, Supplementary Table 17-18). Enrichment Z-scores per cell type for ET genes as well as drug DEGs were calculated based on average normalized expression in single nucleus cerebellum data from Lake et al. (2018)[21] and cortical single-cell Smart-seq data from the Allen Brain Institute. In the cerebellum, ET genes were mostly enriched in astrocytes (enrichment z-score = 3.11, q-value = 0.021; Figure 4A and 4B). In the cortex, the strongest enrichments of ET genes were found in oligodendrocyte progenitor cells (OPCs) (z-score = 3.55) and L3-L5 excitatory neurons with the most significant neuronal cell type being the *FEZF2-, DYRK-* expressing pyramidal neurons of cortical layer V (z-score = 3.28, q-val = 0.0068; Figure 4C). Significant enrichment was also found in L1 *MTG1* astrocytes (z-score = 3.13, q-val = 0.0090).

Next, we assessed the enrichment of propranolol and primidone DEGs identified in this study in cortical and cerebellar single-cell data (Figure 5, Supplementary Table 17-18). In cerebellum single-nucleus data, convergent propranolol DEGs were mostly enriched in endocytes (z-score = 3.38, q-val = 0.014) and microglia (z-score = 3.36, q-val = 0.014) whilst convergent propranolol/primidone DEGs in all cell types were mostly enriched in oligodendrocytes (z-score = 2.90, q-val = 0.034; Figure 5E). Interestingly, convergent propranolol/primidone DEGs in DAOYs, a cell-type specific to the cerebellum, had enriched expression in astrocytes (z-score = 2.74, q-val = 0.047), much like the enrichment of ET genes in cerebellar astrocytes (Figure 4A). In cortical tissue, convergent drug DEGs were mostly significantly enriched in non-neuronal cell types (figure 5D), notably oligodendrocytes (z-score = 5.09, q-val = 3.65E-07), astrocytes (z-score. = 4.92, q-val = 1.00E-04) and endocytes (z-score = 3.95, q-val = 1.70E-03). Unsurprisingly, given

294 the use of propranolol to lower blood pressure, convergent propranolol DEGs were mostly
295 enriched in endocytes (z-score = 6.18, q-val = 4.48-07) and vascular and leptomeningeal cells
296 (VLMC; z-score = 4.77, q-val = 1.52E-04). Of note, propranolol DEGs were also enriched in L1-
297 L3 inhibitory neurons, notably vasoactive intestinal peptide (VIP) expressing inhibitory neurons
298 (Figure 5D, see Supplementary Table 17 and 18 for statistics).
299

300 **DISCUSSION**

301 Understanding the cellular and molecular mechanisms behind drug treatments can inform on
302 disease pathophysiology. In this study, we sought to investigate the transcriptomic effects of first
303 line treatments for ET in cerebellar DAOY cells as well as NPCs, to gain insight on potential
304 disease related genes. We found that propranolol and primidone affected expression of multiple
305 genes related to movement disorders and ET. Notably, *TRAPPC11,* whose expression was
306 previously shown to be altered in ET cerebellar cortex and is also involved in protein trafficking[26].
307 Other genes related to endosomal trafficking were found to be differentially expressed after
308 propranolol treatment, such as *MYO1E* and *SYNJ1*. Convergent DEGs also displayed an
309 enrichment of genes related to the ESCRT complex, known to be a pillar of endosomal trafficking
310 in neurons. These findings potentially increase the likelihood of endosomal trafficking being
311 altered in ET and possibly partly restored through transcriptomic effects of propranolol.
312

313 Axon guidance was previously associated with ET in several studies[2,11,26,34,35]. Bulk-RNA
314 sequencing of cerebellar cortex and dentate nucleus of ET patients showed a significant enrichment
315 of axon guidance genes[26]. Hallmark axon guidance genes such as *ROBO1* (z-score = 5.87, q-val =
316 1.88E-06) and *NEO1* (z-score = 4.01, q-val = 5.04E-03) were both found to have increased

317 expression following drug treatment. NEO1 (and its paralog DCC), which binds netrin-1, is
318 implicated in cell-cell adhesions, mostly between axons and oligodendrocytes, as well as cell-
319 extracellular matrix adhesions. Netrin-1 also acts on dendrite arborisation, increasing connections
320 in excitatory synapses[36]. Interestingly, NEO1 protein remains expressed in Purkinje cells of the
321 adult cerebellum (GTEx V8). Thus, the post-developmental role of axon guidance signalling
322 pathways is to maintain adhesions and important synaptic connections between cells. This might
323 be an important process by which ET tremorolytic drugs diminish tremor. These findings on axon
324 guidance are concordant with other Reactome/GO-terms found to be enriched amongst DEGs,
325 most notably semaphorin interactions, cadherin binding, and actin cytoskeleton reorganization.
326 Purkinje cell axons in ET patients have shown accumulations of disordered neurofilaments
327 ('axonal torpedoes') leading to abnormal axonal morphologies[35]. This process is thought to either
328 be part of a neurodegenerative cascade or a response to neurodegeneration. Moreover, decreased
329 neuronal density was observed in multiple brain regions of ET patients, most notably the inferior
330 cerebellar peduncles through which afferent axons from the brainstem nuclei pass in order to reach
331 the cerebellar cortex[37]. Our findings therefore provide additional support for the involvement of
332 axon guidance molecules in ET pathophysiology.

333

334 We also identified the CaMKK2 signalling pathway as significantly enriched in propranolol DEGs
335 in DAOYs and NPCs. CaMKK2 exacerbates Aβ42 synaptotoxicity in Alzheimer's disease through
336 Tau protein phosphorylation by AMPK[33]. This pathway is sensitive to cellular calcium intake,
337 which was shown to be affected at the transcriptome level by both propranolol and primidone.
338 Both Tau protein and amyloid-beta abnormalities have been observed in ET cerebellar tissues,
339 with multiple findings pointing towards protein aggregation being a hallmark of the disease[38,39].

Propranolol affecting transcription of genes implicated in both CAMKK2 and Ca^{2+} signalling pathways might imply that ET drugs could reduce aggregate-induced neurotoxicity.

Convergent drug DEGs did not correlate with transcriptomic effects of common ET variants (TWAS DEGs). Moreover, propranolol and primidone DEGs displayed weak non-significant correlations with gene expression in the cerebellum of ET patients, the principal brain region affected in this disorder[1]. There are several possible explanations for these results. The relatively underpowered state (for a common disease) of the current ET GWAS might not capture the effects of common variation on transcription, in part explaining the absence of correlation with drug DEGs. Moreover, the lack of good cell models for cerebellar neurons as well as the neurodevelopmental state of NPCs also impair adequate comparisons between TWAS statistics and drug DEGs presented in this study.

Convergent drug DEGs are significantly more likely to be genes predicted to be intolerant to LoF variants. Mutationally constrained genes are more likely to be essential for cell homeostasis and survival and thus more likely to be implicated in disease when affected by LoF mutations[24]. Given that both ET drugs converged on these genes in multiple cell types increases the likelihood that these genes harbour rare variants associated with ET. Upregulated DEGs were found to be significantly less tolerant than all protein coding genes while downregulated DEGs were as tolerant as all protein coding genes. These genes could be good candidates for future targeted sequencing, especially within propranolol and primidone responsive cohorts.

Identifying cell types affected in ET remains difficult. Several conflicting studies have tried to identify specific pathological morphologies in post-mortem cerebellum of ET patients, most notably in Purkinje cells, yet no defining histopathological markers have been found[35]. Here we sought to identify the relevant ET cell types by assessing the enrichment of variant-harbouring ET genes within single cells in cerebellar and cortical tissues. Expression of ET genes were mostly enriched within L3-L5 excitatory neurons in the cerebral cortex, more specifically *FEZF2* L5 glutamatergic pyramidal neurons[40]. These neurons originate in the primary motor cortex (M1) and form the corticospinal tract that projects to lower motor neurons, which controls conscious movements. These neurons are influenced by multiple cortico-cortical pathways but also input from the cerebellothalamic tract, crucial for movement coordination. The primary motor cortex has previously been shown to be important for tremor generation in ET as subdural stimulation of M1 can reduce tremor intensity in patients[41]. Moreover, propranolol-targeted genes were mostly enriched in VIP-expressing inhibitory neurons of L1-L3. These neurons are known to inhibit motor neurons through different cortical pathways[42]. The enrichment of ET genes within M1 pyramidal neurons coupled with the enrichment of ET drug genes in motor neuron-inhibiting cells does suggest new potential cellular mechanisms through which tremor generation (and/or reduction) occurs in ET.

In the cerebellum, both ET genes and convergent drug DEGs were significantly enriched within astrocytes in the cerebellum. This somewhat contradicts previous histopathological findings postulating that Purkinje cells were the defining cell type in ET pathophysiology. Not much is known about the role of astrocytes in ET but based on other neurodegenerative diseases, it could be argued that they may play an important role in the onset or development of the disease[35].

Oligodendrocytes, whose dysfunction contributes to numerous other neurological diseases, also showed an enrichment of propranolol and primidone-targeted genes. Both astrocytes and oligodendrocytes might be targeted by ET drugs to reduce tremor since non-neuronal cell types are known to be involved in neurodegeneration in numerous diseases[43]. The lack of single-cell data on ET tissues is a limitation in the study of this disease but our results highlight a possible role for non-neuronal cells in the cerebellum in ET.

This study has a number of limitations. Propranolol and primidone are known to act on cell excitability and this effect was postulated as being important for tremor reduction in ET. Given that DAOYs and NPCs are non-excitable, it is very hard to assess the electrophysiological effects of these drugs in these cells. Moreover, the electrophysiological effects of drugs on cells are known to influence transcription[44]. This might explain why primidone had such a mild effect on transcription in both DAOYs and NPCs. Cells used in this study do not represent the complete range of of cell types in the cortex and cerebellum. NPCs do not completely replicate neuronal expression and do have a more neurodevelopmental transcriptomic state. DAOYs, on the other hand, are derived from cancerous cells and do have dysregulated expression of genes related to cell division and cell growth. Nevertheless, this study only serves as an ET drug effect screen and remains a steppingstone for more in-depth studies.

Our study identifies multiple cellular and molecular pathways implicated in ET pathophysiology and tremor reduction by both propranolol and primidone. Our findings also suggest a role for genes harbouring potentially rare, deleterious variants associated with ET. Targeted sequencing of these convergent drug genes in case-control cohorts could help to confirm or infirm this hypothesis.

These genes could also be used as biomarkers for propranolol treatment in responsive ET patients. Our results also identify several cell types involved in ET in both cerebellar and cortical tissues. We also identify cell types potentially affected by propranolol and primidone through which tremor might be reduced in ET. Future studies will be needed to further identify the transcriptomic and electrophysiological effects of both drugs, possibly using more representative neuronal models such as iPSC-derived Purkinje cells, non-neuronal cell types as well as motor neurons. Moreover, single-cell experiments studying the transcriptomic effects of ET drugs on patient-derived tissues will be required to understand the complex nature of this disease.

REFERENCES

1. Haubenberger D, Hallett M. Essential Tremor. *N Engl J Med*. 2018;378(19):1802-1810. doi:10.1056/NEJMcp1707928
2. Houle G, Dion PA, Rouleau GA. Molecular Genetics of Essential Tremor. *eLS*. June 2018:1-8. doi:doi:10.1002/9780470015902.a0028103
3. Ruderfer DM, Charney AW, Readhead B, et al. Polygenic overlap between schizophrenia risk and antipsychotic response: A genomic medicine approach. *The Lancet Psychiatry*. 2016. doi:10.1016/S2215-0366(15)00553-2
4. So HC, Chau CKL, Chiu WT, et al. Analysis of genome-wide association data highlights candidates for drug repositioning in psychiatry. *Nat Neurosci*. 2017. doi:10.1038/nn.4618
5. Khayachi A, Ase AR, Liao C, et al. Chronic lithium treatment alters the excitatory/inhibitory balance of synaptic networks and reduces mGluR5-PKC signaling. *bioRxiv*. January 2020:2020.09.18.303578. doi:10.1101/2020.09.18.303578
6. Ferreira JJ, Mestre TA, Lyons KE, et al. MDS evidence-based review of treatments for

essential tremor. *Mov Disord*. 2019. doi:10.1002/mds.27700

7. Morgan MH, Hewer RL, Cooper R. Effect of the beta adrenergic blocking agent propranolol on essential tremor. *J Neurol Neurosurg Psychiatry*. 1973. doi:10.1136/jnnp.36.4.618

8. Langley A, Pope E. Propranolol and central nervous system function: Potential implications for paediatric patients with infantile haemangiomas. *Br J Dermatol*. 2015. doi:10.1111/bjd.13379

9. Laurens C, Abot A, Delarue A, Knauf C. Central effects of beta-blockers may be due to nitric oxide and hydrogen peroxide release independently of their ability to cross the blood-brain barrier. *Front Neurosci*. 2019. doi:10.3389/fnins.2019.00033

10. Liao C, Sarayloo F, Rochefort D, et al. Multiomics Analyses Identify Genes and Pathways Relevant to Essential Tremor. *Mov Disord*. 2020. doi:10.1002/mds.28031

11. Liao C, Sarayloo F, Vuokila V, et al. Transcriptomic changes resulting from STK32B overexpression identifies pathways potentially relevant to essential tremor. *bioRxiv*. 2019. doi:10.1101/552901

12. Jefferson D, Jenner-P., Marsden CD. Relationship between plasma propranolol concentration and relief of essential tremor. *J Neurol Neurosurg Psychiatry*. 1979. doi:10.1136/jnnp.42.9.831

13. Hedera P, Cibulčík F, Davis TL. Pharmacotherapy of Essential Tremor. *J Cent Nerv Syst Dis*. 2013. doi:10.4137/jcnsd.s6561

14. Patro R, Duggal G, Love MI, Irizarry RA, Kingsford C. Salmon: fast and bias-aware quantification of transcript expression using dual-phase inference. *Nat Methods*. 2017;14(4):417. doi:10.1038/NMETH.4197

15. Pimentel H, Bray NL, Puente S, Melsted P, Pachter L. Differential analysis of RNA-seq incorporating quantification uncertainty. *Nat Methods*. 2017. doi:10.1038/nmeth.4324

16. Zaykin D V. Optimally weighted Z-test is a powerful method for combining probabilities in meta-analysis. *J Evol Biol*. 2011. doi:10.1111/j.1420-9101.2011.02297.x

17. Langfelder P, Horvath S. WGCNA: An R package for weighted correlation network analysis. *BMC Bioinformatics*. 2008;9. doi:10.1186/1471-2105-9-559/EMAIL/CORRESPONDENT/C1/NEW

18. P D, S van D, JC H, et al. Improving the diagnostic yield of exome- sequencing by predicting gene-phenotype associations using large-scale gene expression analysis. *Nat Commun*. 2019;10(1). doi:10.1038/S41467-019-10649-4

19. Raudvere U, Kolberg L, Kuzmin I, et al. g:Profiler: a web server for functional enrichment analysis and conversions of gene lists (2019 update). *Nucleic Acids Res*. 2019;(1). doi:10.1093/nar/gkz369

20. Aldinger KA, Thomson Z, Phelps IG, et al. Spatial and cell type transcriptional landscape of human cerebellar development. *Nat Neurosci 2021 248*. 2021;24(8):1163-1175. doi:10.1038/s41593-021-00872-y

21. Lake BB, Chen S, Sos BC, et al. Integrative single-cell analysis of transcriptional and epigenetic states in the human adult brain. *Nat Biotechnol*. 2018;36(1):70. doi:10.1038/NBT.4038

22. Hao Y, Hao S, Andersen-Nissen E, et al. Integrated analysis of multimodal single-cell data. *Cell*. 2021;184(13):3573-3587.e29. doi:10.1016/J.CELL.2021.04.048

23. Hawrylycz MJ, Lein ES, Guillozet-Bongaarts AL, et al. An anatomically comprehensive atlas of the adult human brain transcriptome. *Nat 2012 4897416*. 2012;489(7416):391-

399. doi:10.1038/nature11405

24. Karczewski KJ, Francioli LC, Tiao G, et al. The mutational constraint spectrum quantified from variation in 141,456 humans. *Nature*. 2020. doi:10.1038/s41586-020-2308-7

25. Ho D, Imai K, King G, Stuart EA. MatchIt: Nonparametric Preprocessing for Parametric Causal Inference. *J Stat Softw*. 2011;42(1):1-28. doi:10.18637/JSS.V042.I08

26. Liao C, Sarayloo F, Rochefort D, et al. Multi-omics integration of the phenome, transcriptome and genome highlights genes and pathways relevant to essential tremor. *bioRxiv*. January 2019:580753. doi:10.1101/580753

27. Sahoo PK, Lee SJ, Jaiswal PB, et al. Axonal G3BP1 stress granule protein limits axonal mRNA translation and nerve regeneration. *Nat Commun*. 2018. doi:10.1038/s41467-018-05647-x

28. Mircsof D, Langouët M, Rio M, et al. Mutations in NONO lead to syndromic intellectual disability and inhibitory synaptic defects. *Nat Neurosci*. 2015. doi:10.1038/nn.4169

29. Miyamoto Y, Torii T, Tanoue A, Yamauchi J. VCAM1 acts in parallel with CD69 and is required for the initiation of oligodendrocyte myelination. *Nat Commun*. 2016. doi:10.1038/ncomms13478

30. Lorenz D, Klebe S, Stevanin G, et al. Dopamine receptor D3 gene and essential tremor in large series of German, Danish and French patients. *Eur J Hum Genet*. 2009. doi:10.1038/ejhg.2008.243

31. Arango-Lievano M, Sensoy O, Borie A, et al. A GIPC1-Palmitate Switch Modulates Dopamine Drd3 Receptor Trafficking and Signaling. *Mol Cell Biol*. 2016. doi:10.1128/mcb.00916-15

32. Yoshikawa M, Senzaki K, Yokomizo T, Takahashi S, Ozaki S, Shiga T. Runx1 selectively

regulates cell fate specification and axonal projections of dorsal root ganglion neurons. *Dev Biol*. 2007;303(2):663-674. doi:10.1016/J.YDBIO.2006.12.007

33. G M-C, J C, S P, V C, A M, F P. The CAMKK2-AMPK kinase pathway mediates the synaptotoxic effects of Aβ oligomers through Tau phosphorylation. *Neuron*. 2013;78(1):94-108. doi:10.1016/J.NEURON.2013.02.003

34. Hor H, Francescatto L, Bartesaghi L, et al. Missense mutations in TENM4, a regulator of axon guidance and central myelination, cause essential tremor. *Hum Mol Genet*. 2015. doi:10.1093/hmg/ddv281

35. Louis ED, Faust PL. Essential tremor pathology: neurodegeneration and reorganization of neuronal connections. *Nat Rev Neurol*. 2020. doi:10.1038/s41582-019-0302-1

36. Sun KLW, Correia JP, Kennedy TE. Netrins: Versatile extracellular cues with diverse functions. *Development*. 2011. doi:10.1242/dev.044529

37. Prasad S, Pandey U, Saini J, Ingalhalikar M, Pal PK. Atrophy of cerebellar peduncles in essential tremor: a machine learning–based volumetric analysis. *Eur Radiol*. 2019. doi:10.1007/s00330-019-06269-7

38. E B, C T, É A-L, et al. Accumulation of amyloid-β in the cerebellar cortex of essential tremor patients. *Neurobiol Dis*. 2015;82:397-408. doi:10.1016/J.NBD.2015.07.016

39. Kim SH, Farrell K, Cosentino S, et al. Tau Isoform Profile in Essential Tremor Diverges From Other Tauopathies. *J Neuropathol Exp Neurol*. August 2021. doi:10.1093/JNEN/NLAB073

40. Tantirigama MLS, Oswald MJ, Duynstee C, Hughes SM, Empson RM. Expression of the Developmental Transcription Factor Fezf2 Identifies a Distinct Subpopulation of Layer 5 Intratelencephalic-Projection Neurons in Mature Mouse Motor Cortex. *J Neurosci*.

2014;34(12):4303-4308. doi:10.1523/JNEUROSCI.3111-13.2014

41. Moro E, Schwalb JM, Piboolnurak P, et al. Unilateral subdural motor cortex stimulation improves essential tremor but not Parkinson's disease. *Brain*. 2011;134(7):2096-2105. doi:10.1093/BRAIN/AWR072

42. Pfeffer CK, Xue M, He M, Huang ZJ, Scanziani M. Inhibition of inhibition in visual cortex: the logic of connections between molecularly distinct interneurons. *Nat Neurosci 2013 168*. 2013;16(8):1068-1076. doi:10.1038/nn.3446

43. Vahsen BF, Gray E, Thompson AG, et al. Non-neuronal cells in amyotrophic lateral sclerosis — from pathogenesis to biomarkers. *Nat Rev Neurol 2021 176*. 2021;17(6):333-348. doi:10.1038/s41582-021-00487-8

44. Ribeiro EA, Salery M, Scarpa JR, et al. Transcriptional and physiological adaptations in nucleus accumbens somatostatin interneurons that regulate behavioral responses to cocaine. *Nat Commun 2018 91*. 2018;9(1):1-10. doi:10.1038/s41467-018-05657-9

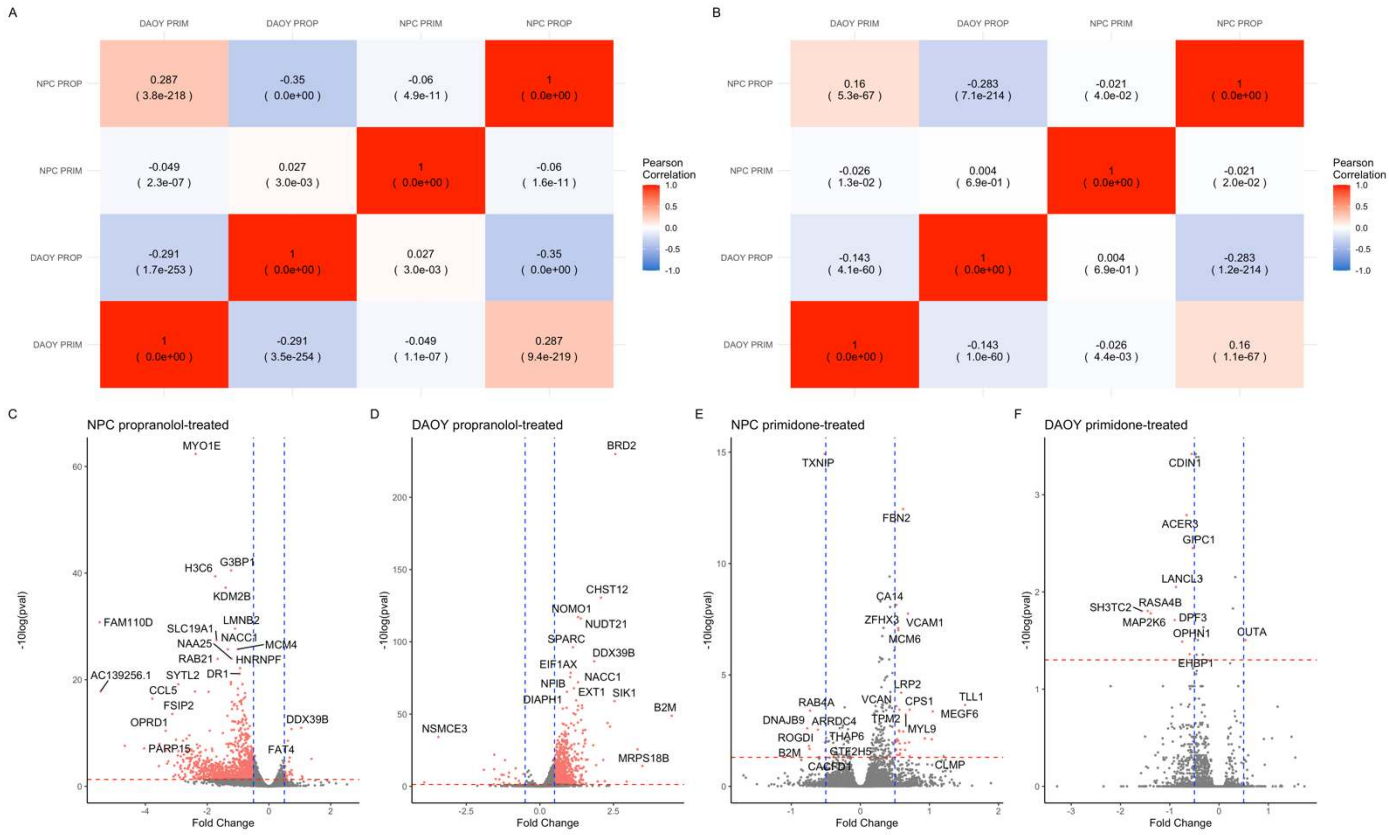

536

537 **Figure 1. Correlation between DAOYs and NPCs treated with propranolol and primidone.**

538 A. Unweighted Pearson correlations between DEGs z-scores from different conditions of

539 treatment and cell types. B. Weighted Pearson correlations between DEGs z-scores from different

540 conditions of treatment and cell types. C-F. Volcano plots of propranolol-treated NPCs (C) and

541 DAOYs (D) as well as primidone-treated NPCs (E) and DAOYs (F). Blue lines indicate -0.5- and

542 0.5-fold changes. Red lines indicate q-value significance threshold (0.05).

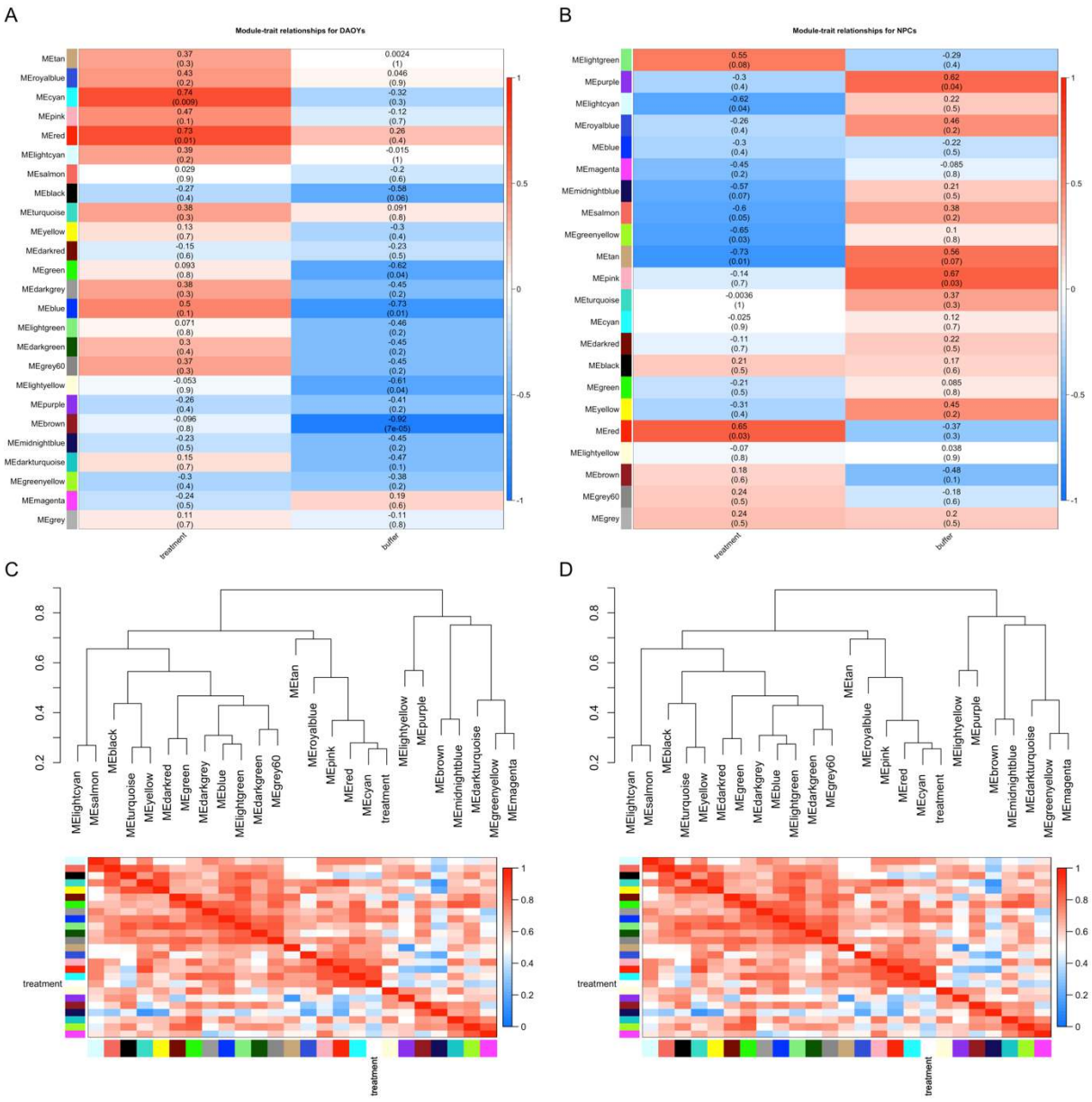

Figure 2. Co-expression gene modules for convergent propranolol and primidone targets. A. Module-treatment (propranolol/primidone) and -buffer (H2O/DMSO; control) correlation heatmaps for DAOYs. B. Module-treatment (propranolol/primidone) and -buffer (H2O/DMSO; control) correlation heatmaps for NPCs. Value indicates correlation between gene-trait and gene-module associations with p-value in parenthesis. C. Module dendrograms with module

549 membership correlation heatmaps for DAOYs. D. Module dendrograms with module membership

550 correlation heatmaps for NPCs.

551

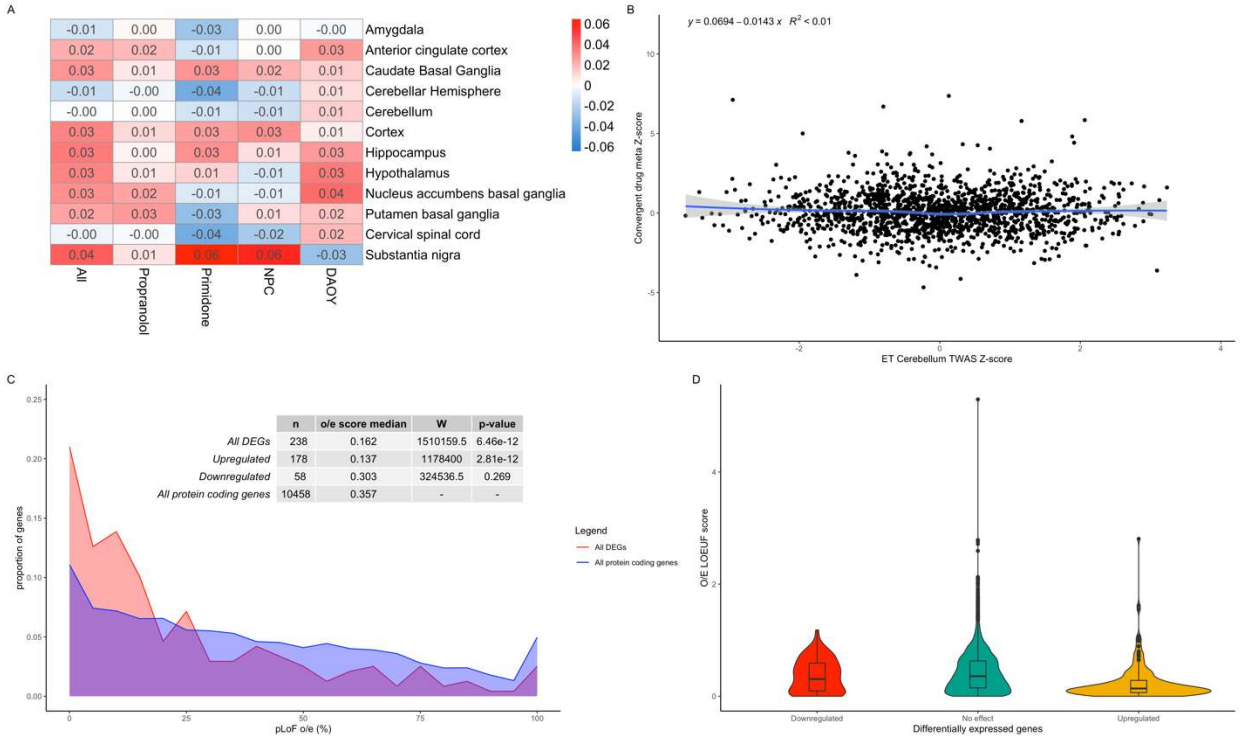

	n	o/e score median	W	p-value
All DEGs	238	0.162	1510159.5	6.46e-12
Upregulated	178	0.137	1178400	2.81e-12
Downregulated	58	0.303	324536.5	0.269
All protein coding genes	10458	0.357	-	-

552

553 **Figure 3. Effects of ET drugs on common and rare variants.** A. Correlation heatmap of ET

554 TWAS gene Z-scores in different brain tissues and drug effect gene Z-scores from different

555 meta-analysis conditions. Values indicate Z-score regression coefficient from linear model. B.

556 Correlation plot of TWAS gene Z-scores from cerebellar tissue and convergent primidone and

557 propranolol gene Z-scores across DAOYs and NPCs. C. Line histogram displaying the

558 distribution of O/E LOEUF scores from all protein coding genes (blue) and convergent DEGs

559 (red) following drug treatment. O/E scores were directly transformed to percentages (ex. 0.25 as

560 25%) with scores over 10 counted as 100%. D. Violin plots of O/E LOEUF scores for

561 upregulated DEGs (yellow), dowregulated DEGs (red) and non-significant DEGs (green).

562

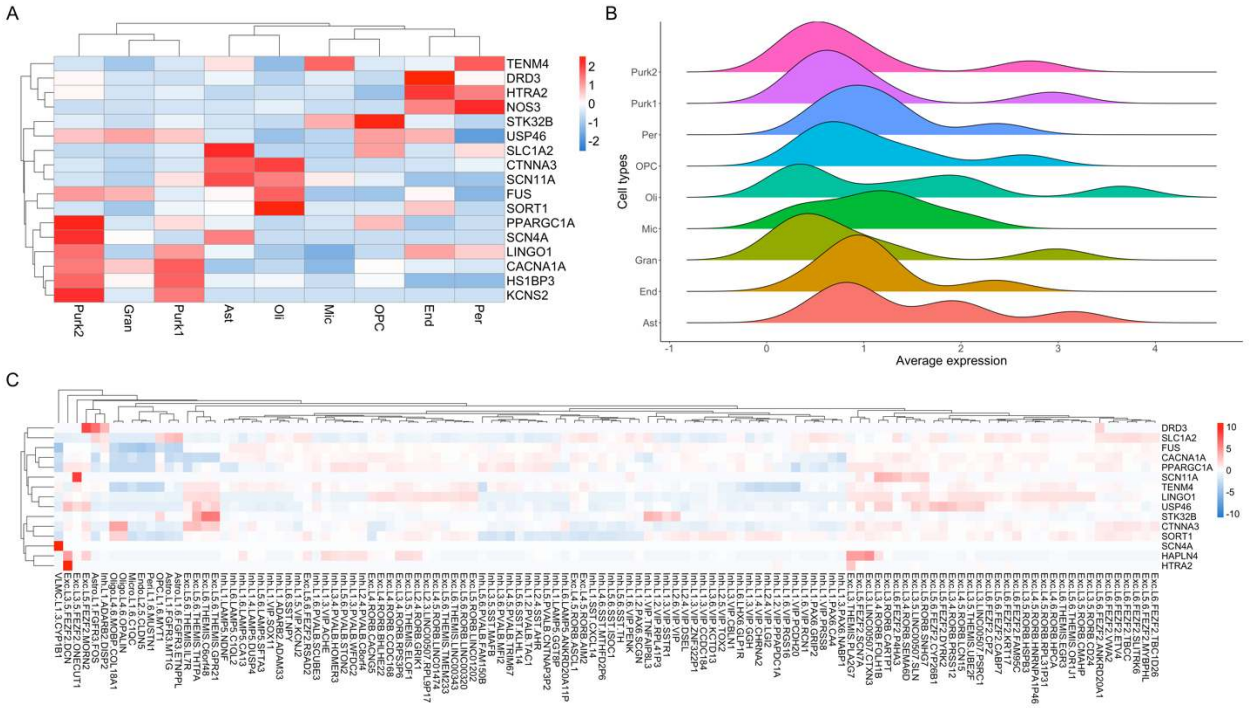

Figure 4. Single-cell enrichment of ET genes in cerebellar and cortical tissues. A. Single-cell enrichment Z-score heatmap of ET-related genes in adult cerebellar tissue. Rows represent ET genes; Columns represent cell types of the cerebellum (Purk1 = SORC3+ Purkinje cells, Purk2 = SORC3- Purkinje cells, Ast = Astrocytes, OPC = Oligodendrocyte progenitor cells, Oli = Oligodendrocytes, Mic =Microglia, End = Endocytes, Gran = Granule cells, Per = Pericytes). B. Ridge plots displaying distribution of average expression counts of ET-related genes in different cell types of the adult cerebellum. C. Z-score expression heatmap of ET genes in single-cell types of the adult cortex. Rows represent ET genes; Columns represent cortical cell types (Exc = Excitatory, Inh = Inhibitory, L# = cortical layer, Astro = Astrocytes).

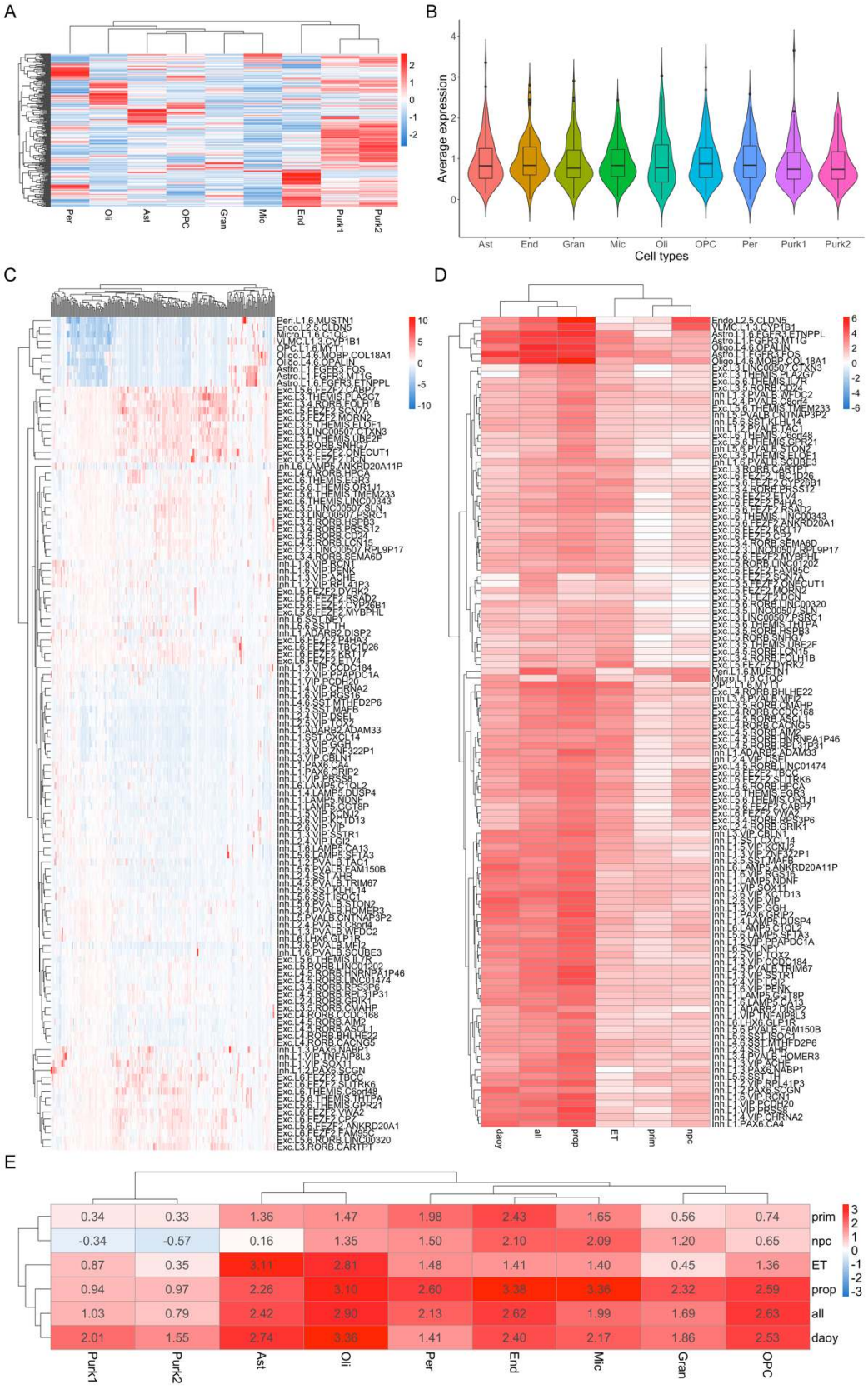

Figure 5. Single-cell enrichment of drug DEGs in cerebellar and cortical tissues. A. Single-cell enrichment Z-score heatmap of convergent propranolol/primidone DEGs in adult cerebellar tissue. Rows represent DEGs; columns indicate cell types; legend color scheme is based on enrichment z-score direction. B. Violin plot of average expression per cerebellar cell type of convergent propranolol/primidone DEGs. C. Single-cell enrichment Z-score heatmap of convergent propranolol/primidone DEGs in adult cortical tissue. Rows represent DEGs; columns indicate cell types; legend color scheme is based on enrichment Z-score direction. D. Enrichment Z-score heatmap of DEGs gene-sets from different conditions (see below for abbreviations) in single-cell data from adult cortex. E. Enrichment Z-score heatmap of DEGs gene-sets from different conditions in single-nucleus sequencing data from adult cerebellar tissue Rows indicate condition gene-sets; columns indicate cerebellar cell-types. Abbreviations: ET, ET related-genes; prop, convergent propranolol DEGs in both cell types; prim, convergent primidone DEGs in both cell types; DAOY, convergent propranolol and primidone DEGs in DAOY cells only; NPC, convergent propranolol and primidone DEGs in NPCs only; all, convergent propranolol and primidone DEGs in both cell types.

Table 1. Pathway enrichment for convergent propranolol DEGs in both DAOYs and NPCs.

SOURCE	TERM	P-VALUE
CORUM	PA700 complex	0.00732592
CORUM	p54(nrb)-PSF-matrin3 complex	0.00741609
CORUM	PA700-20S-PA28 complex	0.01284008
CORUM	HEXIM1-DNA-PK-paraspeckle components-ribonucleoprotein complex	0.05052404
CORUM	Ubiquitin E3 ligase (CHEK1, CUL4A)	0.06576926
CORUM	CORUM root	0.07664168
CORUM	EBAFb complex	0.08852844
CORUM	NCOR1 complex	0.08852844
KEGG	Proteasome	0.00921554
KEGG	Spinocerebellar ataxia	0.02672326
KEGG	Prion disease	0.04664458

KEGG	Protein processing in endoplasmic reticulum	0.05311146
KEGG	Hippo signaling pathway - multiple species	0.08972819
MIRNA	hsa-miR-6766-5p	0.00036715
MIRNA	hsa-miR-6756-5p	0.00036715
MIRNA	hsa-miR-539-5p	0.0003869
MIRNA	hsa-miR-4668-3p	0.00716318
MIRNA	hsa-miR-21-5p	0.0132699
MIRNA	hsa-miR-654-5p	0.02081865
MIRNA	hsa-miR-541-3p	0.02687402
MIRNA	hsa-miR-1468-3p	0.0441487
MIRNA	hsa-let-7b-5p	0.04603661
MIRNA	hsa-miR-548f-5p	0.05118884
MIRNA	hsa-miR-548aj-5p	0.05470749
MIRNA	hsa-miR-548x-5p	0.05470749
MIRNA	hsa-miR-548g-5p	0.05470749
MIRNA	hsa-miR-193b-3p	0.05509061
REAC	Transcriptional regulation by RUNX1	0.00022561
REAC	Oxygen-dependent proline hydroxylation of Hypoxia-inducible Factor Alpha	0.0011874
REAC	Cellular response to hypoxia	0.00350166
REAC	Host Interactions of HIV factors	0.00421087
REAC	Cell Cycle Checkpoints	0.00665026
REAC	UCH proteinases	0.007029
REAC	G2/M Checkpoints	0.01195953
REAC	Regulation of ornithine decarboxylase (ODC)	0.01244161
REAC	G1/S DNA Damage Checkpoints	0.01314543
REAC	Signaling by NOTCH	0.01416007
REAC	p53-Independent G1/S DNA damage checkpoint	0.01463202
REAC	Ubiquitin Mediated Degradation of Phosphorylated Cdc25A	0.01463202
REAC	p53-Independent DNA Damage Response	0.01463202
REAC	Regulation of APC/C activators between G1/S and early anaphase	0.0153801
REAC	Regulation of Apoptosis	0.01714052
REAC	Cdc20:Phospho-APC/C mediated degradation of Cyclin A	0.02113246
REAC	Assembly of the pre-replicative complex	0.02316267
REAC	Deubiquitination	0.02357632
REAC	Autodegradation of Cdh1 by Cdh1:APC/C	0.02437405
REAC	APC:Cdc20 mediated degradation of cell cycle proteins prior to satisfation of the cell cycle checkpoint	0.02451223
REAC	Regulation of MECP2 expression and activity	0.02941481
REAC	Stabilization of p53	0.03112835

REAC	APC/C:Cdc20 mediated degradation of mitotic proteins	0.03270423
REAC	DNA Replication Pre-Initiation	0.03291172
REAC	Orc1 removal from chromatin	0.03381524
REAC	PTEN Regulation	0.03447437
REAC	Metabolism of polyamines	0.03559536
REAC	Activation of APC/C and APC/C:Cdc20 mediated degradation of mitotic proteins	0.03762377
REAC	Regulation of mitotic cell cycle	0.03959616
REAC	APC/C-mediated degradation of cell cycle proteins	0.03959616
REAC	Transcriptional regulation by RUNX3	0.03975456
REAC	CDT1 association with the CDC6:ORC:origin complex	0.04112471
REAC	MAPK6/MAPK4 signaling	0.04224034
REAC	Ub-specific processing proteases	0.04291446
REAC	Switching of origins to a post-replicative state	0.04311326
REAC	APC/C:Cdc20 mediated degradation of Securin	0.045216
REAC	Vpu mediated degradation of CD4	0.05357088
REAC	Cross-presentation of soluble exogenous antigens (endosomes)	0.07194281
REAC	Regulation of activated PAK-2p34 by proteasome mediated degradation	0.07194281
REAC	Hedgehog ligand biogenesis	0.074096
REAC	p53-Dependent G1/S DNA damage checkpoint	0.08163726
REAC	p53-Dependent G1 DNA Damage Response	0.08163726
REAC	SCF-beta-TrCP mediated degradation of Emi1	0.0874049
REAC	CDK-mediated phosphorylation and removal of Cdc6	0.09137813
REAC	Autodegradation of the E3 ubiquitin ligase COP1	0.09544567
REAC	Ubiquitin-dependent degradation of Cyclin D	0.09544567
WP	mRNA Processing	0.00409008
WP	CAMKK2 Pathway	0.00436354
WP	Pathways Affected in Adenoid Cystic Carcinoma	0.01716516
WP	MET in type 1 papillary renal cell carcinoma	0.02394081
WP	Oncostatin M Signaling Pathway	0.07825036
WP	15q13.3 copy number variation syndrome	0.07966433
WP	Gastrin Signaling Pathway	0.09031422

590

591 **Table 2. Pathway enrichment analysis of red gene module for drug treatment in DAOYs**

SOURCE	TERM_NAME	P_VALUE
CORUM	Ubiquitin E3 ligase (CCDC22, COMMD8, CUL3)	0.00491141

CORUM	Ecsit complex (ECSIT, MT-CO2, GAPDH, TRAF6, NDUFAF1)	0.07383335
REAC	TBC/RABGAPs	0.00987381
REAC	RUNX3 regulates YAP1-mediated transcription	0.02324914
REAC	RNA polymerase II transcribes snRNA genes	0.08552303
REAC	Rab regulation of trafficking	0.09310043
WP	Eukaryotic Transcription Initiation	0.09003334

592

593 **Table 3. Pathway enrichment analysis of red gene module for drug treatment in NPCs**

SOURCE	TERM_NAME	P_VALUE
CORUM	AML1-HIPK2-p300 complex	0.01653182
CORUM	EGR-EP300 complex	0.02266982
CORUM	DNA polymerase alpha-primase complex	0.04115007
CORUM	TNF-alpha/NF-kappa B signaling complex 9	0.04269448
GO:BP	cell morphogenesis	9.93E-09
GO:BP	neuron development	4.57E-07
GO:BP	neuron projection development	7.92E-07
GO:BP	cell morphogenesis involved in differentiation	2.46E-06
GO:BP	neuron differentiation	3.78E-06
GO:BP	anatomical structure morphogenesis	5.15E-06
GO:BP	generation of neurons	5.51E-06
GO:BP	neurogenesis	7.43E-06
GO:BP	cell projection morphogenesis	4.04E-05
GO:BP	cellular component morphogenesis	5.32E-05
GO:BP	cell part morphogenesis	8.74E-05
GO:BP	plasma membrane bounded cell projection morphogenesis	0.00010681
GO:BP	nervous system development	0.00011909
GO:BP	neuron projection morphogenesis	0.00017843
GO:BP	cell morphogenesis involved in neuron differentiation	0.00031702
GO:BP	plasma membrane bounded cell projection organization	0.00031755
GO:BP	cell projection organization	0.00043646
GO:BP	morphogenesis of an epithelium	0.00089496
GO:BP	regulation of cell projection organization	0.00122012
GO:BP	tissue morphogenesis	0.0013445
GO:BP	regulation of plasma membrane bounded cell projection organization	0.00156418

GO:BP	regulation of neuron projection development	0.00371164
GO:BP	axon development	0.00411476
GO:BP	cell development	0.00577557
GO:BP	system development	0.00611873
GO:BP	positive regulation of cell projection organization	0.0234741
GO:BP	axonogenesis	0.02708754
GO:BP	regulation of anatomical structure morphogenesis	0.03347413
GO:BP	developmental growth	0.04077868
MIRNA	hsa-miR-218-5p	0.00163474
REAC	Nervous system development	0.01342479
REAC	Axon guidance	0.03273254
REAC	Attenuation phase	0.04873215
WP	Pathways Affected in Adenoid Cystic Carcinoma	0.00025871
WP	Mesodermal Commitment Pathway	0.0277441

594

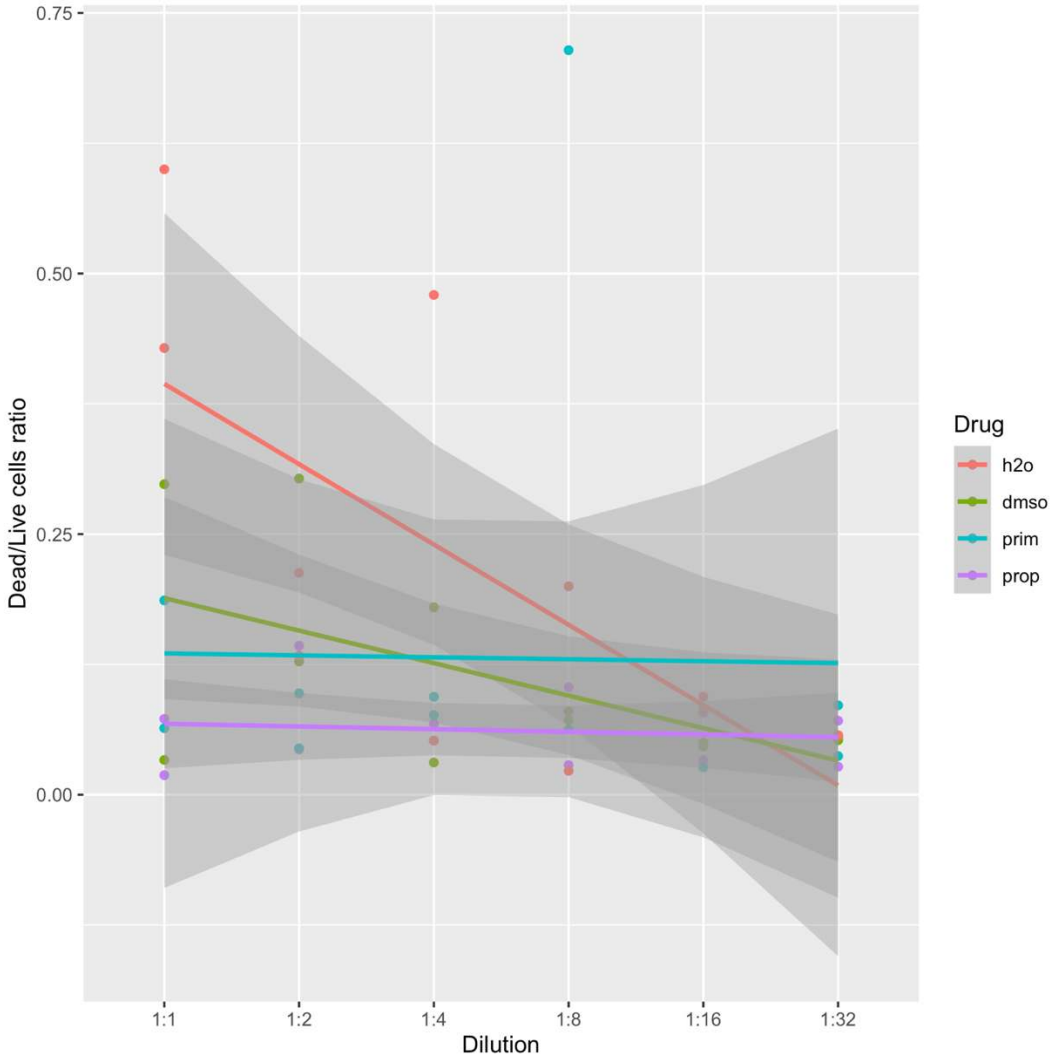

Supplementary Figure 1. DAOY kill curve. Dead over live cell ratios were calculated based on NucGreen and NucBlue (DAPI) staining after 5 days of treatment. Dilutions are calculated from initial concentrations of drugs or DMSO (%; corresponding to the percentage of DMSO that primidone was diluted in). 1:1 dilutions; Propranolol = 0.0156 µg/mL, Primidone = 25 µg/mL; DMSO = 0.235%.

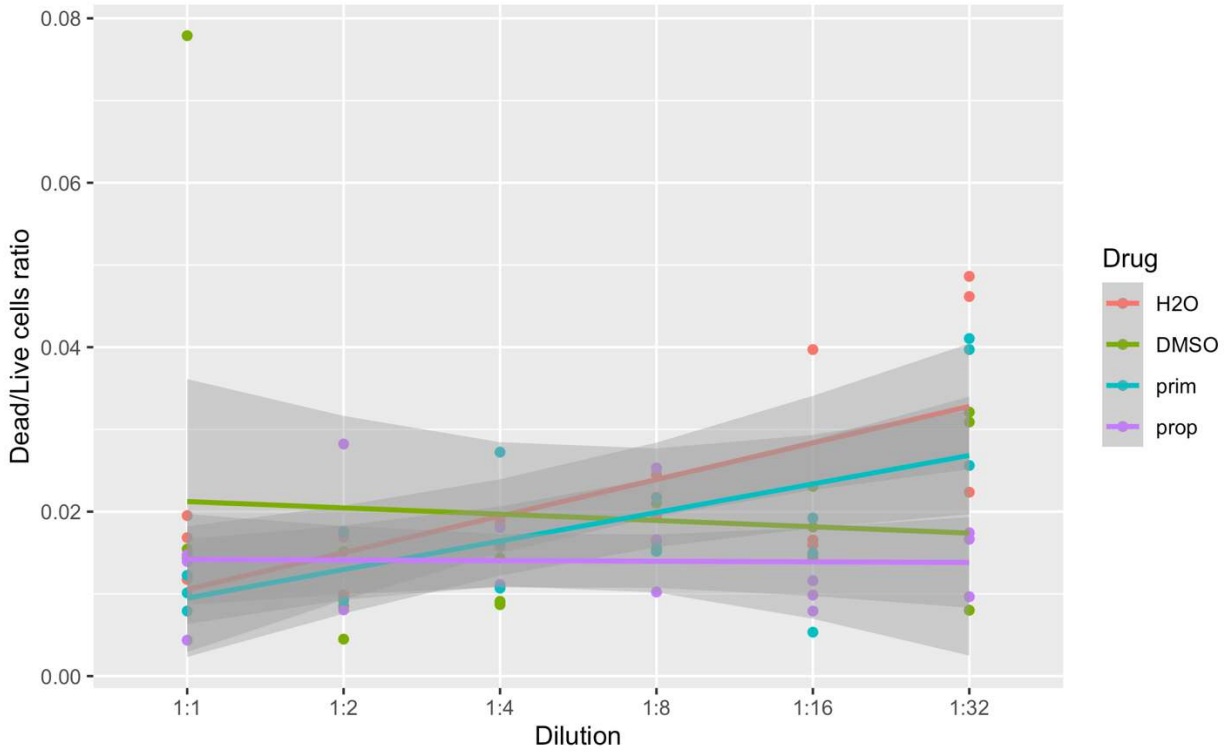

602

603 **Supplementary Figure 2. NPC kill curve.** Dead over live cell ratios were calculated based on
604 NucGreen and NucBlue (DAPI) staining after 5 days of treatment. Dilutions are calculated from
605 initial concentrations of drugs or DMSO (%; corresponding to the percentage of DMSO that
606 primidone was diluted in). 1:1 dilutions; Propranolol = 0.0156 µg/mL, Primidone = 25 µg/mL;
607 DMSO = 0.235%.

608

609

610

611

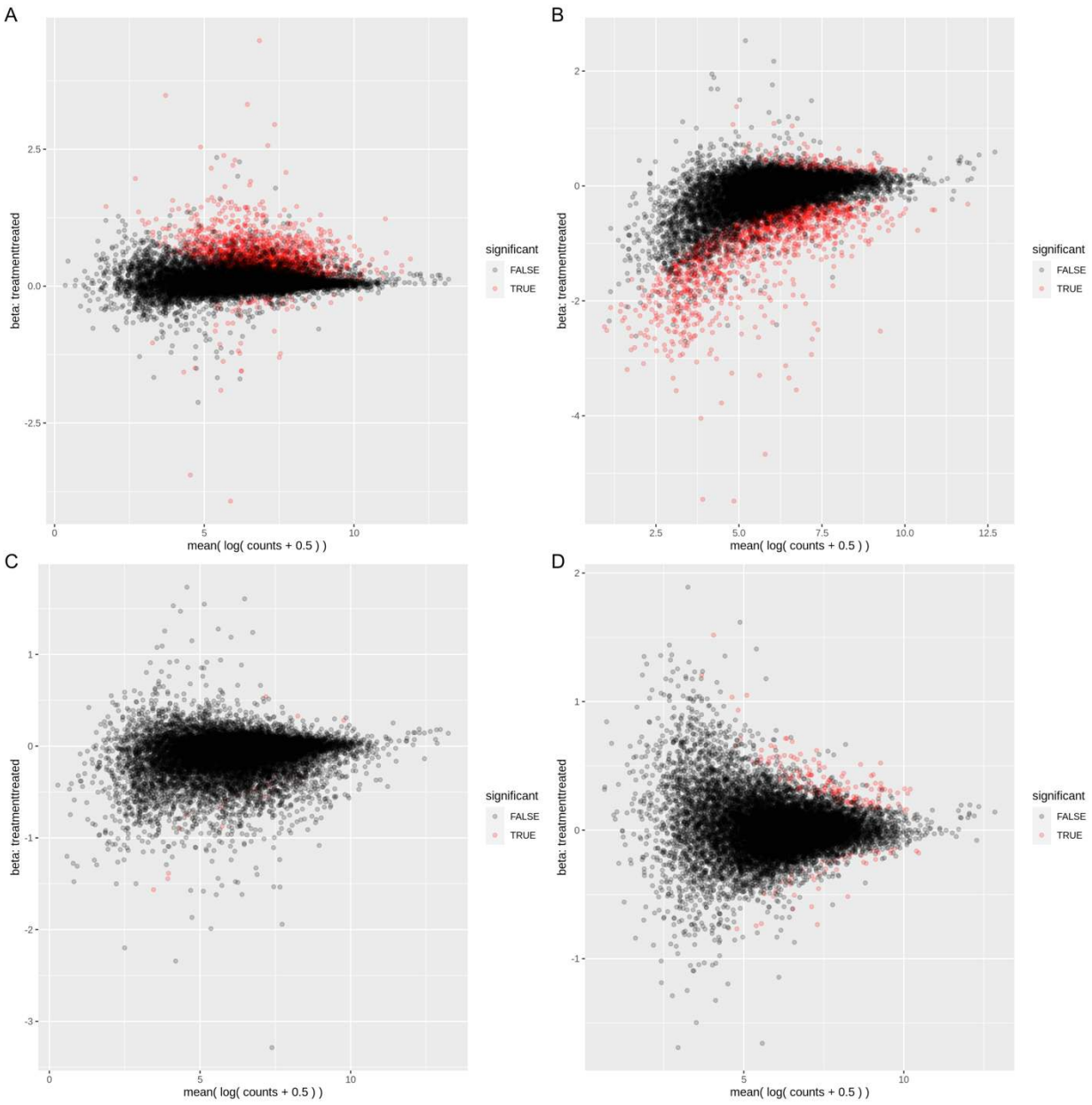

Supplementary Figure 3. Mean A plots. A. DAOYs treated with propranolol. B. DAOYs treated with primidone. C. NPCs treated with propranolol. D. NPCs treated with primidone

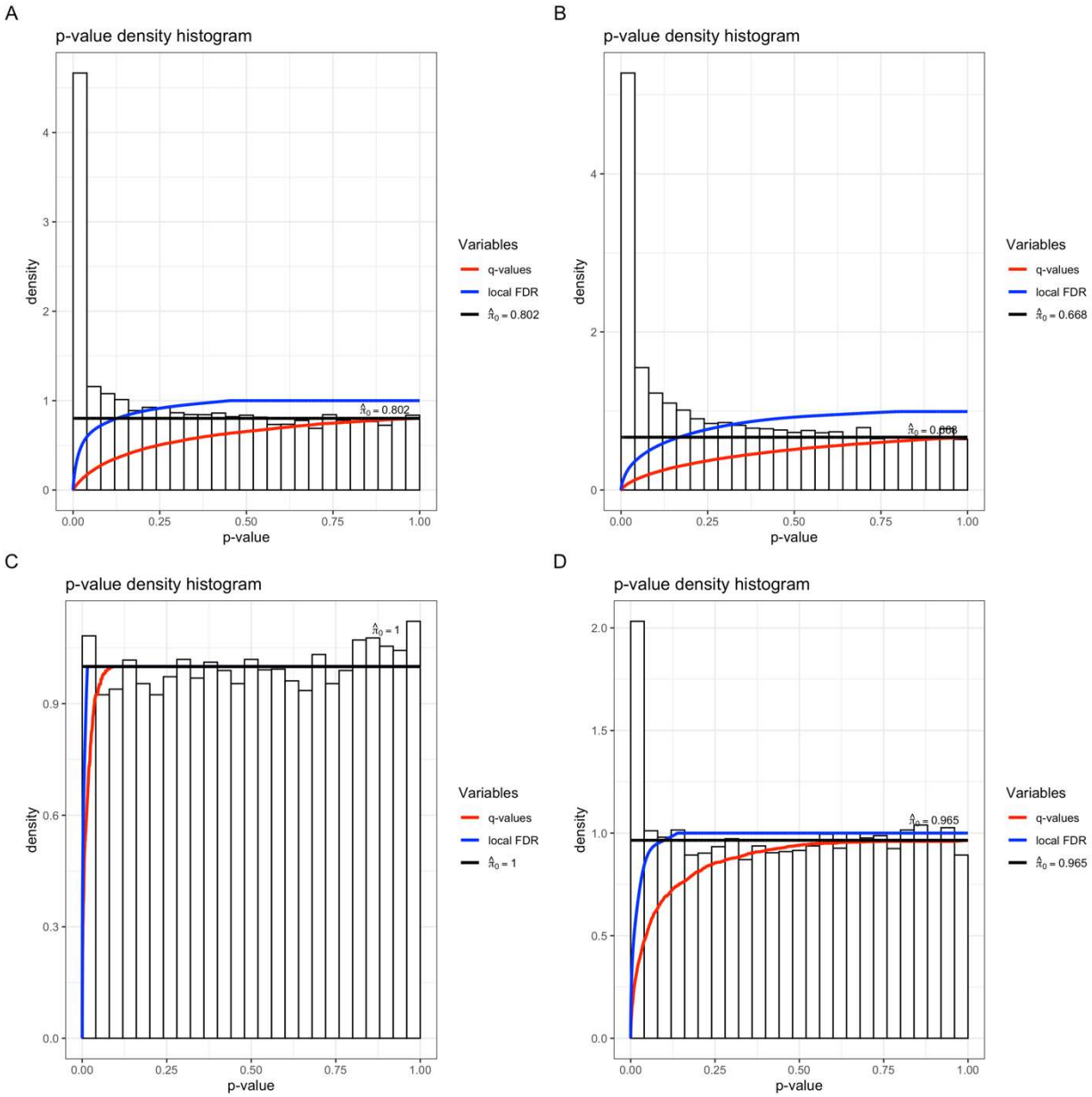

615

616 **Supplementary Figure 4. P-value histograms.** A. DAOYs treated with propranolol. B. DAOYs

617 treated with primidone. C. NPCs treated with propranolol. D. NPCs treated with primidone.

618

619